

International conference on applications of
physics to medicine and biology. Trieste
(Italy) - 30 Mar - 3 Apr 1982

CEA-CONF--6214

Proton nuclear scattering radiography. by J. SAUDINOS

ABSTRACT

Nuclear scattering of protons allows to radiograph objects with specific properties : 3-dimensional radiography, different information as compared to X-ray technique, hydrogen radiography. Furthermore the nuclear scattering radiography (NSR) is a well adapted method to gating techniques allowing the radiography of fast periodic moving objects. Results obtained on phantoms, formalin fixed head and moving object are shown and discussed. The dose delivery is compatible with clinical use, but at the moment, the irradiation time is too long between 1 and 4 hours. Perspectives to make the radiograph faster and to get a practical method are discussed.

1. INTRODUCTION

Various ways of using high energy protons beams for radiography have been considered and tried in the last decade. They relied mostly on the following mechanisms : Coulomb scattering [1] or measurement of the energy loss and its rapid change near the end of the range [2]. These methods are based on the electromagnetic interaction and measures at one time, one projection. To obtain tomographic information, like in the X-ray scanner, one has to repeat the measurements under a considerable number of angles. The latest development done at Los Alamos [3] arrived to the conclusion of a definite dose advantage for the proton range method as compared with X-rays. In 1975, nuclear scattering radiography [4] was introduced : it relies to strong nuclear interaction and measures directly the density inside elementary volumes. So one of its attractive features is to yield a three-dimensional view of the density distribution without any relative rotation or displacement of the beam and the object.

2. CHARACTERISTICS OF NUCLEAR SCATTERING RADIOGRAPHY (NSR)

When protons in the 1 GeV energy range are incident on an object, most of them go through with a very small angular deviation due to

1015-26

multiple Coulomb scattering and a little energy loss. Some of the particles, however, have strong nuclear interaction with the nucleons (proton and neutron) bound in the nuclei of the atoms of the object. The binding energies of these nucleons, of the order of a few MeV, are relatively small with respect to the energy of impinging protons, and the collision called quasi-elastic, has nearly the character of an elastic encounter between particles of the same mass. So the angular deviation of the incident particle is big : the useful range is 15-40 degrees.

By measuring the trajectories of the incoming and outgoing charged particles, one obtains the three space coordinates of the interaction vertices whose density distributions reflects the matter distribution in the bombarded body (Figure 1). So one obtains directly 3-D radiography without moving the incident beam or the object.

The number of protons scattered by a volume element is directly proportional to the nuclear quasi-elastic cross section σ . Its dependence on the atomic mass A is very different from that of X-rayon particle transmission coefficients because in these cases the basic interaction is electromagnetic. So NSR gives different information : for exemple, calcium in bone do not give a screening effect.

We call the radiographs obtained by measuring only the incident and scattered trajectories simple radiographs, by opposition to the hydrogen radiographs which we discuss now. When an incident proton encounter a nucleon it may transfer to it enough energy to leave the target. If it is a proton, it can be detected.

There is a fundamental difference on the properties of this recoil proton if the scattering happens on a hydrogen atom or on any other element : in the second case, before the interaction the recoil nucleon bound in its nucleus has a random Fermi momentum distribution. In case of hydrogen because the nucleus is made only of one proton, it is at rest and kinematical laws lead to two constraints : the scattered and recoil protons are co-planar with the incident proton, the angles θ_1 and θ_2 of the two outgoing protons with respect to the direction of the incoming one obey the relation : $\text{tg}\theta_1 \times \text{tg}\theta_2 = \text{constant}$. Applying these criteria [5], RDN is able to obtain 3-D radiography of the hydrogen content in objects.

3. EXPERIMENTAL METHOD

A detailed discussion of the experimental set-up shown on Figure 1 can be found elsewhere [6]. The incident beam (Z-axis) goes through two scintillation counters SC1, SC2 and two localization multiwire proportional chambers [7] CH1-CH2 perpendicular to it (X-Y plane). After the target two localization chambers CH3-CH4 and a scintillation counter SC3 detect the scattered particle. If there is a recoil proton, it is localized by CH3. Fast time coincidence SC1-SC2 (10 ns) allows to count the number of incident protons and to know the dose delivered during the irradiation. Fast time coincidence SC1-SC2-SC3 (10 ns) defines a scattering event and triggers the reading of the four localization chambers. CH1 and CH2 have an area of $20 \times 20 \text{ cm}^2$ and define the field of radiography. Their localization precision is about 0.6 mm. They give the coordinates X_1, Y_1 and X_2, Y_2 of the points where the incident trajectory cross them. Chambers CH3 and CH4 have an area of $100 \times 100 \text{ cm}^2$ and allow the localization of scattered particles up to an angle of 40° . Their localization precision is about 2 mm. They give the coordinates X_3, Y_3 and X_4, Y_4 of the points where the scattered trajectory cross them. Furthermore, if a recoil proton leaves the target, the coordinates X_5, Y_5 of its intersection with CH3 are measured. The typical intensity of the proton beam is about 3×10^5 particles per second. Because the memory time of the localization chambers is only 200ns, the scattered trajectory is associated with the corresponding incident one. A coding system reads the eight or ten coordinates and transfers them to a fast computer called SAR [8]. The reading and transfer time is of the order of 1 μs . The SAR computes the coordinates XR, YR, ZR of the intersection in space of the incident and scattered straight lines defined X_1Y_1, X_2Y_2 and X_3Y_3, X_4Y_4 . It is directly coupled to a mass memory of 2.1 millions of 12 bits elements. This memory is used as a three dimensional matrix X, Y, Z, typical dimensions being 160, 160, 80. Each element of the mass memory corresponds to an elementary volume (voxel) of the target defined by : $\Delta V = \Delta X \times \Delta Y \times \Delta Z$. $\Delta X, \Delta Y, \Delta Z$ are chosen in function of the localization resolution of the system. Typical values are 0.6 or 1.2 mm for ΔX and ΔY , 2.4 mm for ΔZ . When one event satisfies the conditions, $X \leq XR < X + \Delta X, Y \leq YR < Y + \Delta Y, Z \leq ZR < Z + \Delta Z$, the SAR adds one count to the voxel of address X, Y, Z. All of these operations takes

now about 50 μ s to be completed. In case of hydrogen radiography, the SAR has also to compute the two kinematical criteria and it takes about 100 μ s to analyse one event. Because the SATURNE accelerator in Saclay gives a burst of 500 ms of protons each second, we are presently able to measure about ten thousands scattered events per second in case of simple radiography. With this acquisition rate, after an irradiation of four hours, the mass memory contains about one hundred millions of scattered events. For each voxel, the number of events is proportional to the density and to the nuclear cross sections of the corresponding target voxel. The 3-D matrix is stored on a magnetic tape and has to be corrected for various parasitic effects : lack of uniformity of the intensity of the incident beam, differential absorption of particles in large targets, variations of the solid angle of detection. It is possible also by smoothing techniques to decrease the statistical fluctuations and to improve the sensitivity at the cost of a loss in spatial resolution. To visualize the 3-D matrix, one shows successions of adjacent slices in three orthogonal planes : perpendicular to the beam (slice XY), vertical parallel to the beam (slice ZY) or horizontal (slice ZX). The width of the slices and the size of the picture element (pixel) may be varied by grouping several volume elements. A gray scale is used with the highest pixel value being white and the lowest black. To increase the contrast of the radiographs, one may subtract a constant quantity.

4. EXPERIMENTAL RESULTS

After the first works [4,5] done at CERN in 1975, it appeared that if the properties of the RDN were attractive, a severe limitation for a practical use was the low data acquisition rate which corresponds to very long time of irradiation. In 1977, at Saclay an experiment [9] done with human tissues showed the capability of the method to clearly separate the spinal cord from the formalin solution inside a spine segment either in simple or hydrogen radiography. At the same time, trials on copper, lead and uranium specimens showed the interest of the RDN to radiography heavy materials [10]. However, the acquisition rate was very low 16 millions of events being recorded during an eight day irradiation. In 1978, at CERN, a further step [11] toward the practical exploitation of the method was made. A human head preserved in a formalin

solution was investigated and during a four days irradiation, one hundred and thirty millions of simple events and seven millions of hydrogen events were recorded. The accuracy of the localizations of the particles was about 1 mm for the X and Y coordinates and about 4 mm for the Z one. The volumic resolution taking in account the uncertainty due to the multiple Coulomb scattering was estimated to be about 5 mm^3 . For the 3D-matrix, the dimensions of X, Y, Z equal to 124, 124, 96 with $\Delta X = \Delta Y = 1.4 \text{ mm}$ and $\Delta Z = 2.8 \text{ mm}$. So the voxel was 5.5 mm^3 . About 100 scattered events were stored per voxel for soft tissues and the dose delivery was 0.3 rad. The results of simple radiographs are shown on Figures 2,3,4 and a comparison between hydrogen and simple radiography is done on Figure 5. Four adjacent planes have been summed so the voxel is 22 mm^3 . The 3D-matrix is visualized in three orthogonal planes : X-Y slices on Figure 2 correspond to the horizontal plane of the head going from the level of the nose (Z=33-36) to the level of the occiput (Z=81-84). On these radiographs, bone appears in white and soft tissues in different grays. The slices 69-72 and 73-76 shows very clearly two hypo-densities in the two brain hemispheres. These hypo-densities were also visualized by X-ray CT. Z-X slices on Figure 3 correspond to frontal planes of the head. The hypo-densities in the upper part of the brain appears clearly on different slices. The slice Y=85-88 goes through the part of the spine attached to the head. Z-Y slices on Figure 4 correspond to the sagittal planes of the head. On Figure 5, we compare horizontal slices obtained in simple and hydrogen radiography. In the latter case, bone appears in blacks because it does not contain very much hydrogen (6 % in weight compared to 11 % for soft tissue). On slice 69-72, the hypo-density of the upper part of the brain appears nicely in hydrogen radiography in spite of a worse statistical precision : it appears that the brain hypo-density corresponds to a contrast of 5 % in simple radiography and 15 % in hydrogen radiography.

These results showed the interesting features of the RDN and demonstrated once more, the need for a shorter irradiation time.

In 1980, at Saclay we began to run the experimental system described in part 2 and still applied it to the radiography of a human head. Its position with respect to the incident beam was so that XY slices correspond to sagittal plane. During a ten hours irradiation one hun-

dred and forty millions of simple events were recorded and analysed. Dimensions X, Y, Z of the 3-D matrix was equal to $160 \times 160 \times 80$ width $\Delta X = \Delta Y = 1.27$ mm, $\Delta Z = 2.54$ mm corresponding to a voxel of 4 mm^3 . About 250 scattered events were stored per voxel for soft tissues and the dose delivery was about one rad. The result is presented on Figure 6. Five adjacent elementary slices have been summed so the voxel is 20 mm^3 . Part of the formalin solution leaked out of the head so the different anatomical parts of the brain appear very clearly. During the last year, we improved our data acquisition rate and during an irradiation of one hour, we recorded about 25 millions of events. We tried to point out the spatial resolution and we choosed $\Delta X = \Delta Y = 0.635$ mm and $\Delta Z = 2.54$ mm corresponding to a voxel of 1 mm^3 . About 10 events per mm^3 were stored for soft tissues. On Figure 7, four adjacent planes have been summed. The pixel is 0.4 mm^2 and the width of the slice 10 mm. On slice $Z=31-34$, one can see very clearly the optic nerve going to the sella turcica.

5. PROSPECTS OF THE NSR

NSR has demonstrated some of its interesting features :

- easy 3-D radiography,
- good spatial resolution : this is specially true for sagittal planes which cannot be obtained directly by X-ray scanners,
- possibility of hydrogen radiography,
- delivered dose compatible with clinical use.

Furthermore it appeared that NSR is well adapted to gating technique allowing the radiography of periodically moving objects. In Saclay, we did the radiography of a moving electric motor (1800 revolutions/minute). For medical application, this could be interesting for heart radiography.

But there is still a severe limitation because a too long irradiation time. Presently, we need about four hours to do a radiography. During this year, we plan to gain a factor two to three by allowing the SAR to compute the vertices in a permanent way. To go faster, we will have to change all our experimental set-up because it will appear a new limitation due to the increase of the intensity of the incident beam going throught the large chambers CH3 and CH4. So to detect the

scattered and recoil particles, we plan to use two sets of two chambers out of the beam and parallel to it. Associated with a new version of our computer, this would allow to increase the data acquisition speed by a factor 10. In that conditions, we could probably do a radiograph in 15 minutes.

It will take about two years to get this new system working.

REFERENCES

- [1] West, D. and Scherwood, A.C., *Nature* 239, 157 (1972).
- [2] Steward, V.W. and Koehler, A.M., *Radiology* 110, 217 (1974).
- [3] Hanson, K.M., Bradbury, J.N., Koeppe, R.A., Macek, R.J., Machen, D.R., Morgado, R., Paciotti, M.A. and Sandford, S.A., *Phys. Med. Biol.* 26, 965 (1981).
- [4] Saudinos, J., Charpak, G., Sauli, F., Townsend, D. and Vinciarelli, J., *Phys. Med. Biol.* 20, 890 (1975).
- [5] Charpak, G., Majewski, S., Perrin, Y., Saudinos, J., Sauli, F., Townsend, D. and Vinciarelli, J., *Phys. Med. Biol.* 21, 941 (1976).
- [6] Duchazeaubeneix, J.C., Thèse d'Université, Université Paris-Sud, Centre d'Orsay (1982).
- [7] Charpak, G., Bouclier, R., Bressani, T., Favier, J. and Zupancic, C., *Nucl. Instr. Meth.* 62, 262 (1968).
- [8] Bricaud, B., Faivre, J.C. and Pain, J., *IEE Trans. Nucl. Sci.* NS26, 4641 (1979).
- [9] Berger, J., Duchazeaubeneix, J.C., Faivre, J.C., Garreta, D., Legrand, D., Rouger, M., Saudinos, J., Raybaud, C. and Salamon, G. *J. Comput. Assist. Tomogr.* 2, 488 (1978).
- [10] Duchazeaubeneix, J.C., Faivre, J.C., Garreta, D., Guillerminet, B., Legrand, D., Rouger, M., Saudinos, J. and Berger, J., *Materials Evaluation* 37, 76 (1979).
- [11] Duchazeaubeneix, J.C., Faivre, J.C., Garreta, D., Guillerminet, B., Rouger, M., Saudinos, J., Palmieri, P., Raybaud, C., Sabamon, G., Charpak, G., Melchart, G., Perrin, Y., Santiard, J.C. and Pauli, F. *J. Comput. Assist. Tomogr.*, 4, 803 (1980).

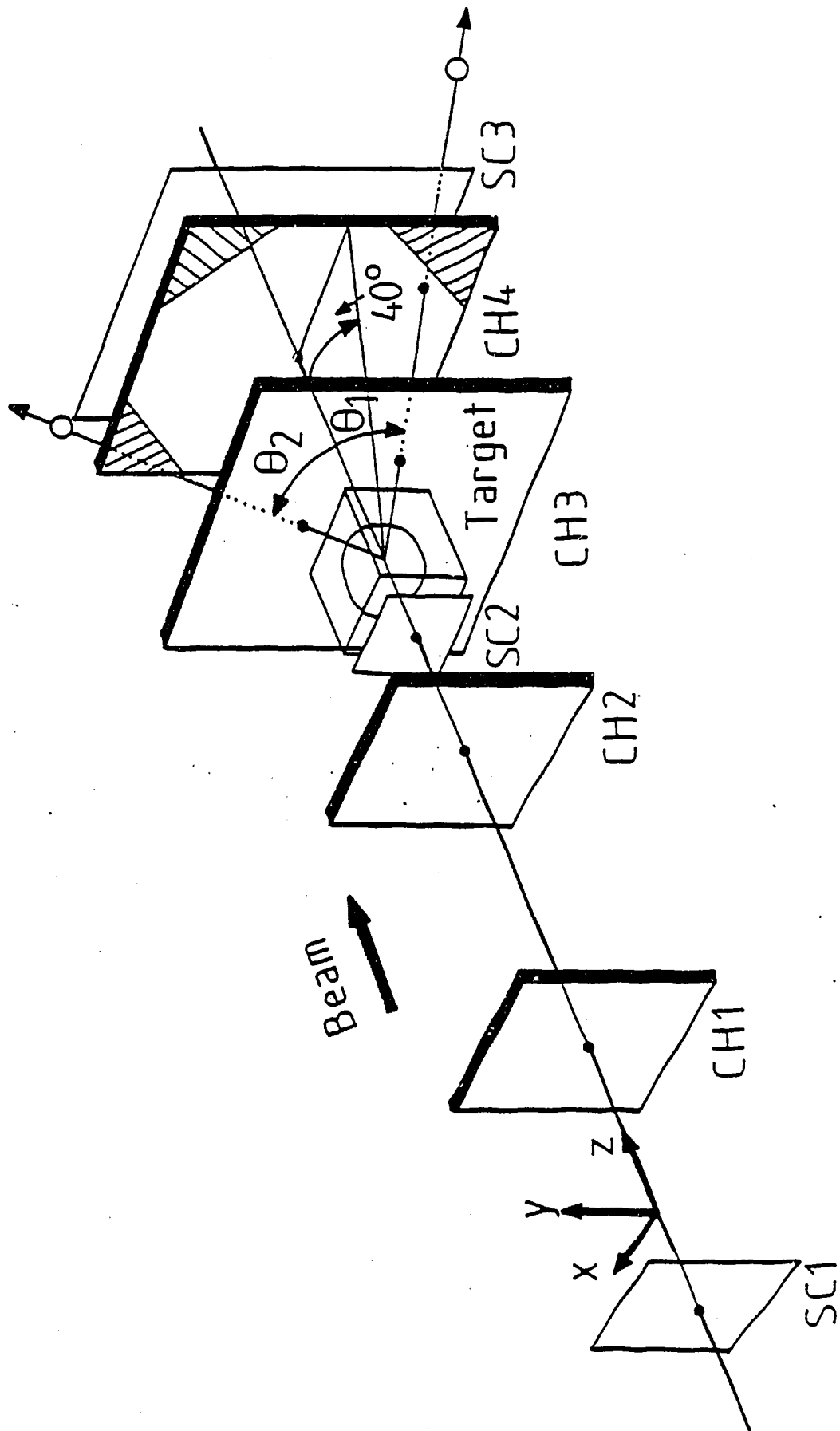


Figure 1 - Layout of the apparatus for nuclear scattering radiography.

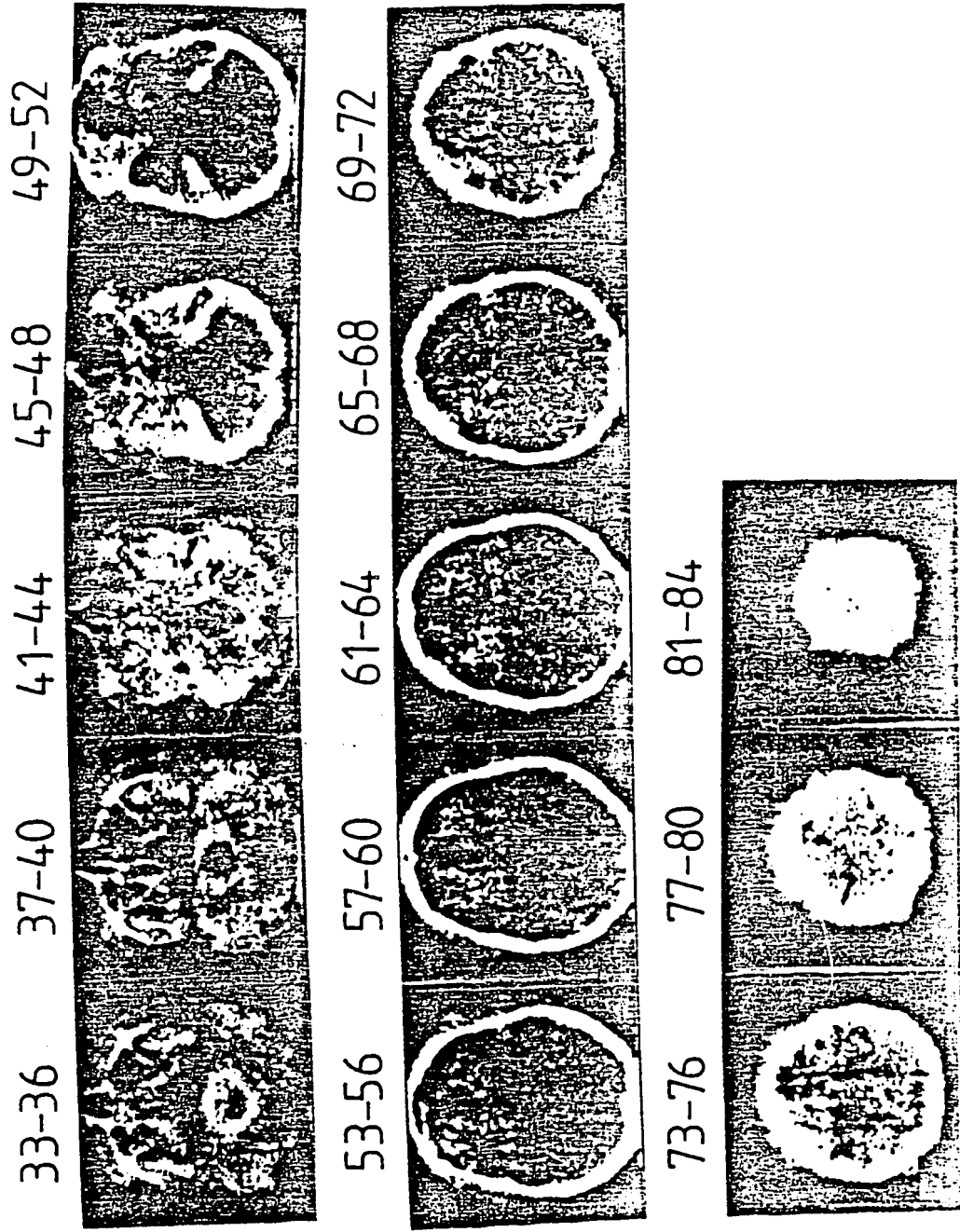


Fig. 2 - Successive horizontal slices (X-Y plane) of a human head obtained by simple NSR. Pixels are $1.4 \times 1.4 \text{ mm}^2$ and slice width 11 mm. Numbers give the Z coordinate of the slice. The dose delivery is 0.3 rad for a four days irradiation done at CERN in 1978.

65-68 69-72 73-76 77-80 81-84



85-88 89-92 93-96 97-100 101-104

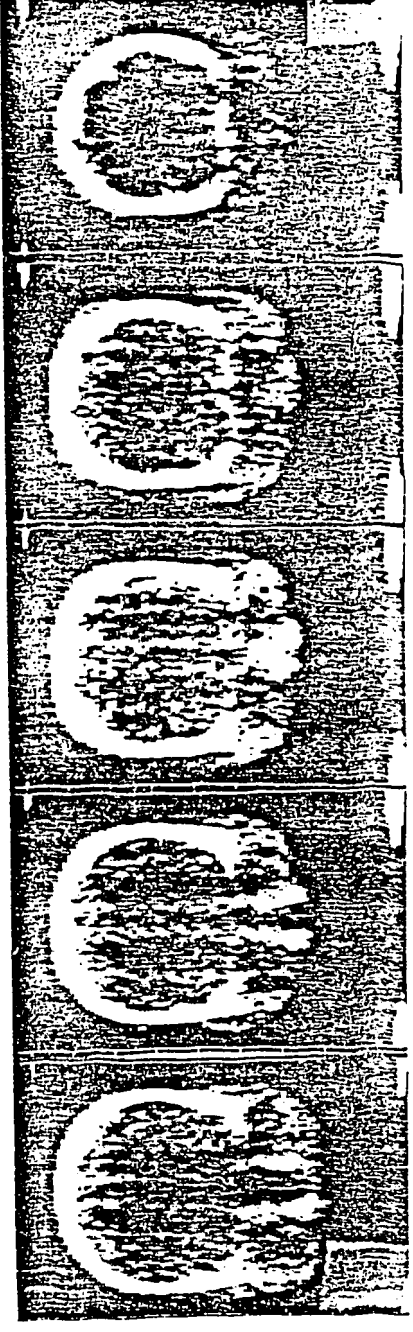


Figure 3 - Successive frontal slices (Z-X plane) obtained during the same radiography. Pixels are $2.8 \times 1.4 \text{ mm}^2$ and slice width is 5.6 mm. Numbers give the Y coordinate of the slice.

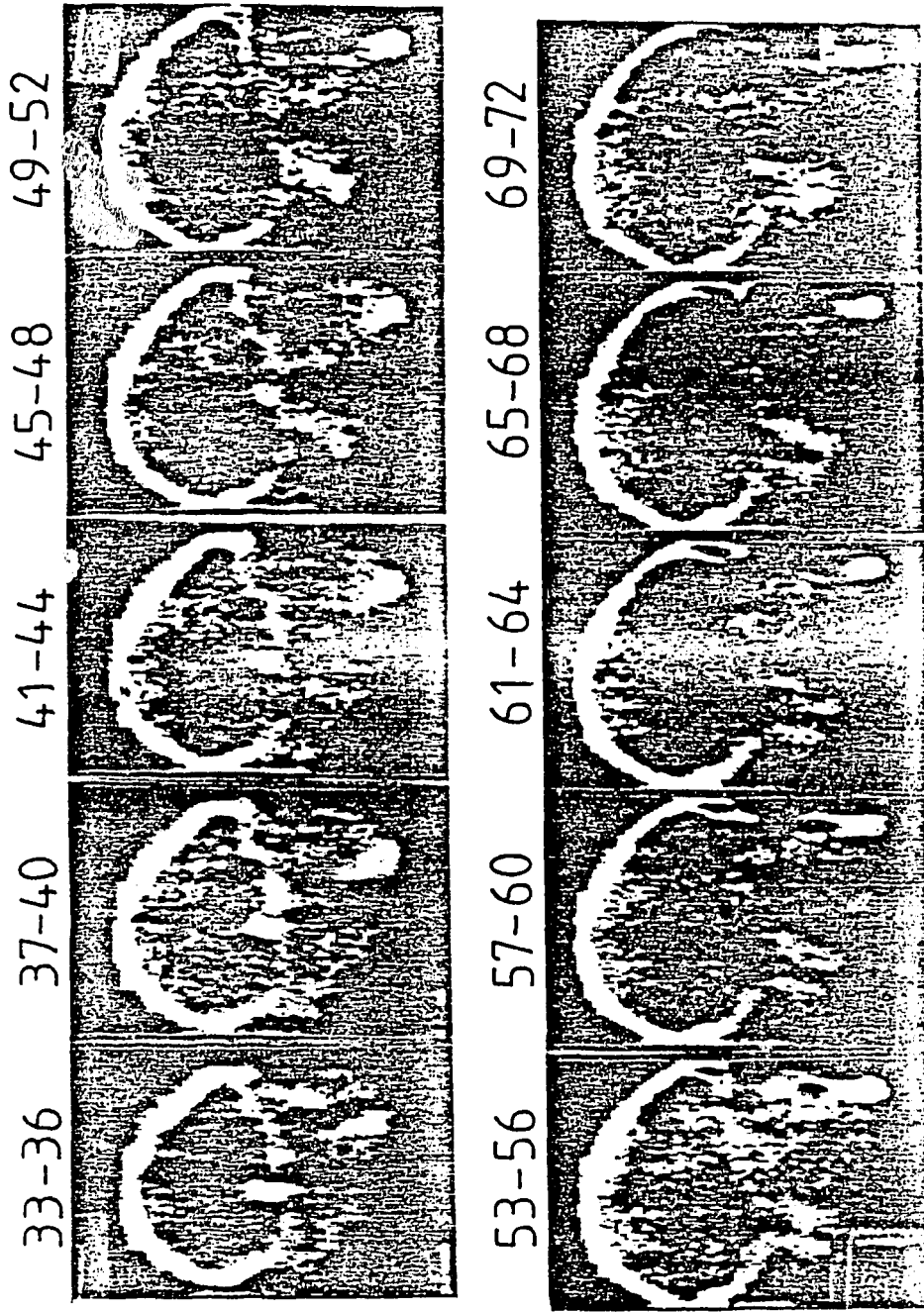


Figure 4 - Successive sagittal slices (X-Y plane) obtained during the same radiography. Pixels are $2.8 \times 1.4 \text{ mm}^2$ and slice width is 5.6 mm. Numbers give the X coordinate of the slice.

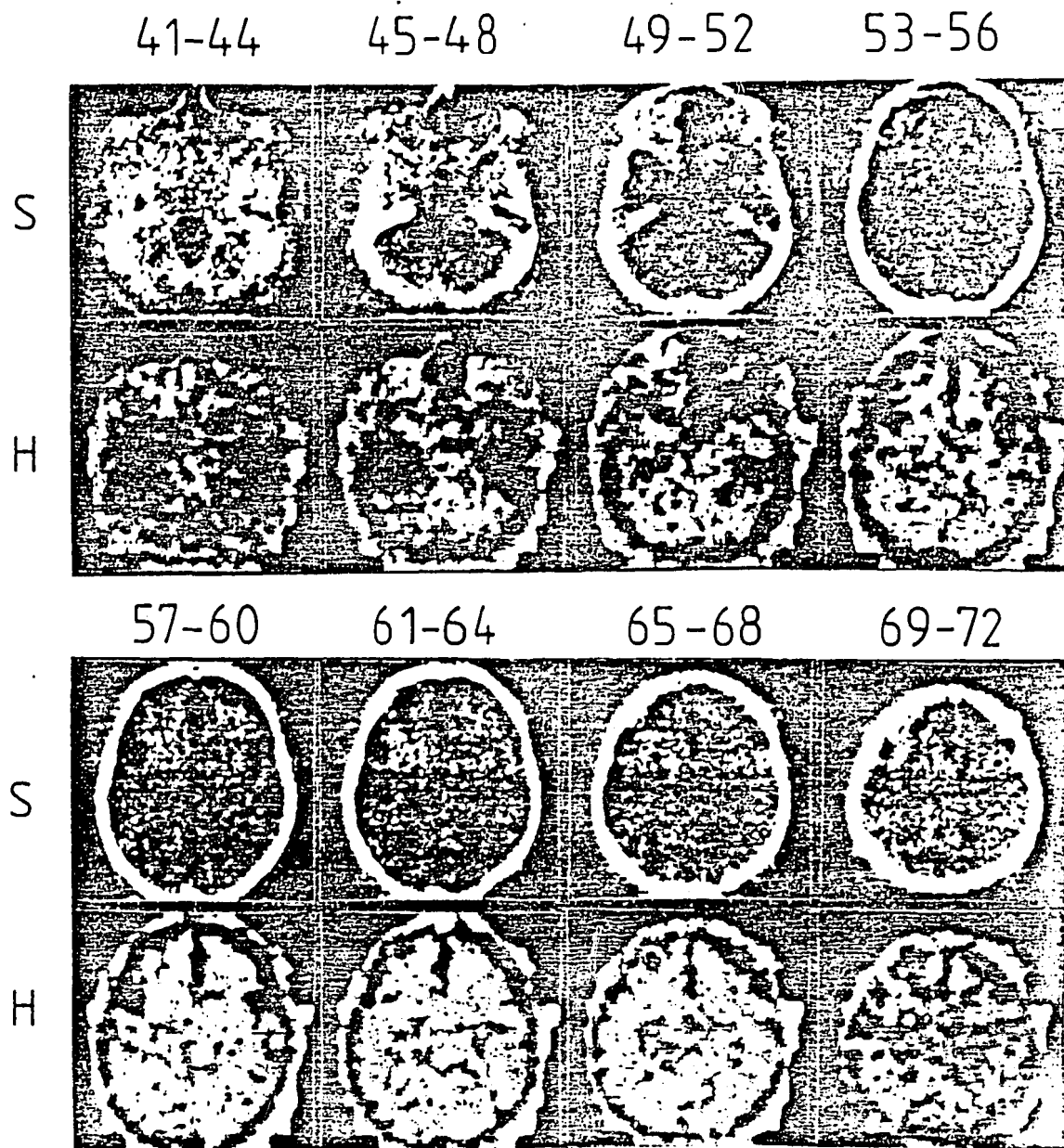
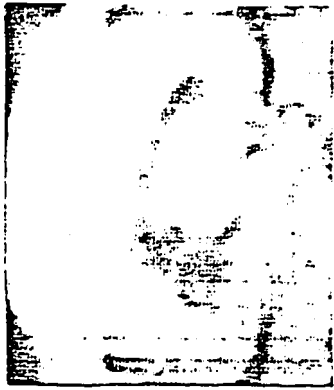
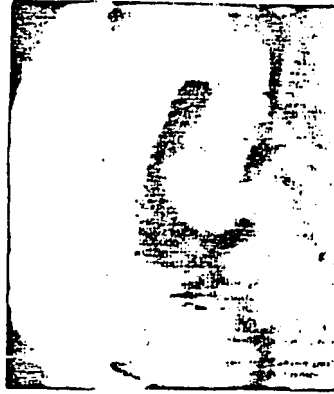


Figure 5 - Comparison of horizontal slices (X-Y plane) obtained simultaneously by simple and hydrogen NSR. Numbers give the Z coordinate of the slice : simple radiograph correspond to S line and hydrogen radiograph to H line.

Z=27-31



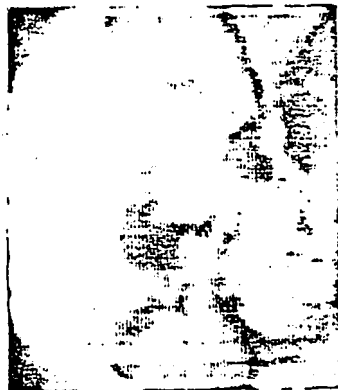
Z=32-36



Z=37-41



Z=42-46



Z=47-51



Z=52-56

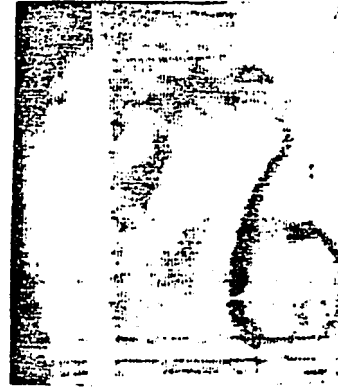


Figure 6 - Successive sagittal slices (X-Y plane) obtained by simple NSR of a human head. Pixels are 1.27×1.27 mm² and slice width is 12.7 mm. Numbers give the Z coordinate of the slice. The dose delivery is about 1 rad for a ten hours irradiation done at Saclay in 1980.

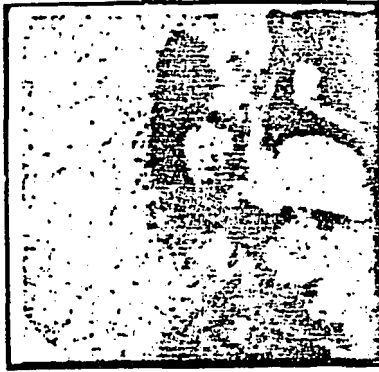
TR 23_26



TR 27_30



TR 31_34 (Plan médian)



TR 35_38



TR 39_42



TR 43_46



Figure 7 - Successive sagittal slices (X-Y planes) obtained by simple NSR of a human head. Pixels are $0.635 \times 0.635 \text{ mm}^2$ and slice width is 10 mm. Numbers give the Z coordinate of the slice. The irradiation done at Saclay in 1981 lasted one hour.